Monthly Notices
of the
ROYAL ASTRONOMICAL SOCIETY

MNRAS **503,** 1319–1326 (2021)
Advance Access publication 2021 February 25

doi:10.1093/mnras/stab519

The velocity dispersion function of early-type galaxies and its redshift evolution: the newest results from lens redshift test

Shuaibo Geng,[1]★ Shuo Cao,[1]★ Yuting Liu,[1] Tonghua Liu,[1] Marek Biesiada[1,2] and Yujie Lian[1]

[1]*Department of Astronomy, Beijing Normal University, Beijing 100875, China*
[2]*National Centre for Nuclear Research, Pasteura 7, PL-02-093 Warsaw, Poland*

Accepted 2021 February 19. Received 2021 February 19; in original form 2021 January 1

ABSTRACT

The redshift distribution of galactic-scale lensing systems provides a laboratory to probe the velocity dispersion function (VDF) of early-type galaxies (ETGs) and measure the evolution of ETGs at redshift $z \sim 1$. Through the statistical analysis of the currently largest sample of ETG gravitational lenses, we conclude that the VDF inferred solely from strong lensing systems is well consistent with the measurements of SDSS DR5 data in the local Universe. In particular, our results strongly indicate a decline in the number density of lenses by a factor of two and a 20 per cent increase in the characteristic velocity dispersion for the ETG population at $z \sim 1$. Such VDF evolution is in perfect agreement with the ΛCDM paradigm (i.e. the hierarchical build-up of mass structures over cosmic time) and different from 'stellar mass-downsizing' evolutions obtained by many galaxy surveys. Meanwhile, we also quantitatively discuss the evolution of the VDF shape in a more complex evolution model, which reveals its strong correlation with the number density and velocity dispersion of ETGs. Finally, we evaluate if future missions such as LSST can be sensitive enough to place the most stringent constraints on the redshift evolution of ETGs, based on the redshift distribution of available gravitational lenses.

Key words: gravitational lensing: strong – galaxies: evolution – galaxies: formation – cosmology: observations.

1 INTRODUCTION

The formation and evolution of early-type galaxies (ETGs) have been the focus of many observational studies, because they can provide more robust tests of the underlying Λ cold dark matter (ΛCDM) theory. Meanwhile, one of the most interesting problems of the ETGs is to determine their velocity dispersion function (VDF), which can provide clues to galaxy formation and evolution. In the last decade, the wealth of data from large sky surveys such as Sloan Digital Sky Survey (SDSS; Abazajian et al. 2009) enabled the determination of the fundamental VDF parameters at different scales, based on the spectroscopic measurements of stellar kinematics within the effective radius, as well as the extended X-ray-emitting gas temperature extended to the dark halo. Specifically, in the local Universe the VDF has been measured using direct kinematic measurements from the SDSS spectroscopic data of ETGs (Sheth et al. 2003; Choi et al. 2007). However, for a given large sample of galaxies such as the SDSS sample, accurately classifying large numbers of galaxies is the major difficulty in deriving reliable type-specific VDF (Chae 2007). The low-velocity dispersion bias should also be appropriately corrected, i.e. in the magnitude-limited catalogues the galaxy number counts become incomplete at low-velocity dispersions (Bernardi et al. 2010). On the other hand, the shape and redshift evolution of the VDF carries information about the physical mechanisms responsible for the growth of a galaxy. For instance, the central gas accretion and the resulting star formation could efficiently increase the velocity dispersion and mass, while mass-loss in galactic winds could play a different role. The evolutions of the VDF from a high-redshift Universe are not understood as well, although ETGs, especially massive elliptical galaxies, are commonly thought to be the end results of the galaxy merging and accretion processes (Kauffmann, White & Guiderdoni 1993; Cole et al. 1994; Kauffmann 1996) (however see Renzini 2006 for a far more complicated history). Observational evidence of such scenarios can be directly compared to predictions from cosmological simulations, based on the SDSS luminosity functions and intrinsic correlations between luminosity and velocity dispersion (Chae 2010).

Independent of the traditional redshift surveys, in this work, we constrain the VDF of ETGs using the statistics of strong gravitational lensing systems (Turner et al. 1984; Biesiada 2006; Cao et al. 2012b,c). Assuming the concordance cosmological model (ΛCDM), several efforts have been made to include the distribution of lensed image separations in the study of the galaxy mass profiles and the evolution history of galaxies. Based on the CLASS and PANELS lens sample, the first attempt to constrain the redshift evolution of galaxies (since redshift $z \sim 1$) was presented in Chae & Mao (2003). This study was then extended to the study of the shape of the VDF and the characteristic velocity dispersion (Chae 2005). However, the sample size of the data available at that time did not allowed for a firm determination of the galaxy VDF. Here, we present a new approach to derive the VDF based on the lens redshift distribution (Kochanek 1992) and to constrain its evolution out to $z \sim 1$, given its strong dependency on the dynamical properties of galaxies (i.e. stellar velocity dispersion) and the number density of gravitational lenses (i.e. galaxy evolution). Compared with the previous works

★ E-mail: gengshuaibo@mail.bnu.edu.cn (SG); caoshuo@bnu.edu.cn (SC)

focusing on image separation distributions, constraining a VDF through lens redshift test is unique and promising, since it does not require the knowledge of the total lensing probability and the magnification bias in the sample (Ofek, Rix & Maoz 2003). The advantages of the lens redshift test have been extensively discussed in Matsumoto & Furamase (2008), Koopmans et al. (2009), Oguri et al. (2012), and Cao et al. (2012a). Therefore, it will be rewarding to investigate the VDF and evolution of the lensing galaxies by adopting the cosmological parameters determined by *Planck* and using a new lens sample better representing the distribution of the galaxy properties. In this work, we focus on a newly compiled sample of 157 galaxy-scale strong lensing systems, which are all early-type lenses (E or S0 morphologies) without significant substructures or close companion galaxies (Chen, Li & Shu 2019). Throughout the paper, we assume the concordance cosmology by adopting the cosmological parameters determined by the *Planck* 2016 data (Ade et al. 2016).

2 METHODOLOGY AND OBSERVATIONAL DATA

Because ETGs dominate the lensing cross-sections due to their large central mass concentrations (Keeton & Kochanek 1997), one may naturally expect them being a unique mass-selected sample to study the VDF and evolution of galaxies, which has triggered numerous efforts to use early-type galactic lenses for this purpose. We mostly follow the methodology described in Ofek et al. (2003) and Cao et al. (2012a) to calculate the lensing probabilities for the lens sample, although a number of modifications and updates are included for more accurate calculations. Based on the number density of the lens $n(\theta_{\rm E}, z_l)$ and the lensing cross-section $S_{\rm cr}$ for multiple imaging, the differential probability that a source with redshift $z_{\rm s}$ will be multiply imaged with Einstein radius $\theta_{\rm E}$ by a distribution of galaxies per unit redshift can be defined by

$$\frac{{\rm d}\tau}{{\rm d}z_l} = n(\theta_{\rm E}, z_l)(1+z_l)^3 S_{\rm cr}\frac{c{\rm d}t}{{\rm d}z_l}. \tag{1}$$

Here, the lensing cross-section and the proper distance interval are, respectively, expressed as

$$S_{\rm cr} = \pi\theta_{\rm E}^2 D_l^2, \tag{2}$$

and

$$\frac{c{\rm d}t}{{\rm d}z_l} = \frac{c}{(1+z_l)}\frac{1}{H(z_l)}, \tag{3}$$

with $H(z)$ and D_l representing the expansion rate of the Universe at redshift z and the angular diameter distance between the observer and the lens. In this paper, following the method proposed by Ofek et al. (2003), we use the differential optical depth for lensing with respect to the lens redshift z_l as the probability density. Then the relative probability of finding the early-type lens at redshift z_l for a given source with Einstein radius $\theta_{\rm E}$ is derived as

$$\delta p = \frac{{\rm d}\tau}{{\rm d}z_l}/\tau = \frac{{\rm d}\tau}{{\rm d}z_l}/\int_0^{z_s}\frac{{\rm d}\tau}{{\rm d}z_l}{\rm d}z_l. \tag{4}$$

(i) The VDF of galaxies (or the lens number density) is an essential part of the theoretical prediction of the lensing probability. Assuming a power-law relation between luminosity (L) and velocity dispersion (σ), the distribution of ETGs in velocity dispersion can be described by the modified Schechter function

$$\frac{{\rm d}n}{{\rm d}\sigma} = n_*\left(\frac{\sigma}{\sigma_*}\right)^{\alpha}\exp\left[-\left(\frac{\sigma}{\sigma_*}\right)^{\beta}\right]\frac{\beta}{\Gamma(\alpha/\beta)}\frac{1}{\sigma}, \tag{5}$$

where n_* is the integrated number density of galaxies, and σ_* is the characteristic velocity dispersion. The shape of VDF is characterized by the low-velocity power-law index (α) and the high-velocity exponential cut-off index (β). Note that α and β are not only used as important input to the strong lensing statistical analysis, but they also contribute towards revealing the features of the distribution of ETGs. Thus, in this paper, an independent method – the redshift information of the lensing galaxies – will be used to place constraints on the VDF shape parameters. We also consider the possibility of redshift evolution of the velocity function through a parametric approach, which is supported by the high-resolution N-body simulation following the evolution of 512^3 particles in a cosmological box of $100h^{-1}$ Mpc (Jing & Suto 2002). More specifically, the evolutions of the number density and the velocity dispersion are parametrized as

$$n_*(z_l) \rightarrow n_*(1+z_l)^{\nu_n}, \sigma_*(z_l) \rightarrow \sigma_*(1+z_l)^{\nu_v}, \tag{6}$$

which is a power-law evolution model extensively discussed in the previous analysis of lens statistics (Chae & Mao 2003; Matsumoto & Furamase 2008; Oguri et al. 2012). The no-evolution model is quantified by ($\nu_n = \nu_v = 0$) and has been adopted in most of previous studies, while the cases of ($\nu_n < 0$, $\nu_v > 0$) and ($\nu_n > 0$, $\nu_v < 0$) correspond to two different views of number and mass evolution in the early-type population from $z = 0$ to 1. In this paper, we also focus on another typical redshift evolution model proposed by Ofek et al. (2003) and Chae (2010), which allows the number density of galaxies and the velocity dispersion to vary with redshift as

$$n_*(z_l) \rightarrow n_* 10^{Pz_l}, \sigma_*(z_l) \rightarrow \sigma_* 10^{Qz_l}. \tag{7}$$

Here, P and U are two constant quantities to be determined from the redshift distribution of galactic-scale lensing systems (see the 'Discussion' section for details).

(ii) The lens potential is assumed to originate from a spherically symmetric power-law mass distribution $\rho \sim r^{-\gamma}$ (Treu et al. 2006; Cao et al. 2015; Pan et al. 2016; Qi et al. 2019), in the framework of which the characteristic Einstein radius can be expressed as

$$\theta_{\rm E*} = \lambda(e)\left[4\pi\left(\frac{\sigma_{\rm ap}}{c}\right)^2\frac{D_{\rm ls}}{D_{\rm s}}{\theta_{\rm ap}}^{\gamma-2}f(\gamma)\right]^{\frac{1}{\gamma-1}}. \tag{8}$$

Here, $D_{\rm ls}$ and $D_{\rm s}$ are the angular diameter distances between lens-source and observer-source, respectively. Note that $\lambda(e)$ denotes a dynamical normalization factor (Keeton, Kochanek & Falco 1998), $f(\gamma)$ is a function of the radial mass profile slope, and $\sigma_{\rm ap}$ is the luminosity averaged line-of-sight velocity dispersion inside the aperture $\theta_{\rm ap}$ (Cao et al. 2015). The power-law model can be derived by solving the spherical Jeans equation analytically assuming that stellar and total mass distributions follow the same power-law and velocity anisotropy vanishes (Koopmans et al. 2005), which has been widely used in several studies of lensing events caused by ETGs (Treu & Koopmans 2002; Treu et al. 2006; Cao et al. 2016, 2020, 2021). In this analysis, we adopt the latest constraints on the average logarithmic density slope, based on the direct total-mass and stellar-velocity dispersion measurements from a large sample of secure strong gravitational lens systems (Koopmans et al. 2009). Considering the three-dimensional shapes of lensing galaxies one can take the normalization factor as a mean of two equally probable extreme cases (oblate and prolate): $\lambda(e) = 0.5\lambda_{\rm obl}(e) + 0.5\lambda_{\rm pro}(e)$, where the partial normalization factors are parametrized in the form of (Oguri et al. 2012), with the ellipticity derived from the axial ratio distributions of ETGs in the SDSS survey (Bernardi et al. 2010).

In this paper, following the method proposed by Ofek et al. (2003), we use the differential optical depth to lensing with respect to the lens redshift z_l as the probability density. For a statistical sample that

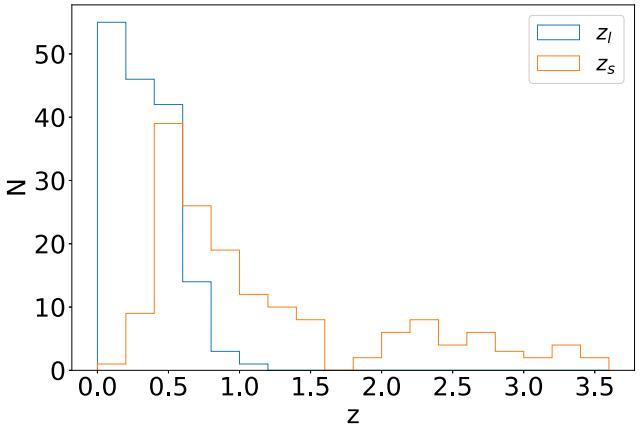

Figure 1. The scatter plot of 158 strong lensing systems used in the lens redshift test.

contains N_l strong lensing systems, the log-likelihood of observing the lens at redshift z_l is given by

$$\ln\mathcal{L}(\mathbf{p}) = \sum_{i=1}^{N_l} \ln\delta p_i(\mathbf{p}), \tag{9}$$

where $\mathbf{p}$ represents the set of the VDF parameters (α, β) and the galaxy evolution parameters (ν_n, ν_v). Now one can perform Monte Carlo simulations of the posterior likelihood $\mathcal{L} \sim \exp(-\chi^2/2)$, where the χ^2 function is defined as

$$\chi^2 = -2\ln\mathcal{L}. \tag{10}$$

in our statistical analysis of lens redshift distribution. The sample used in this paper is primarily drawn from Sloan Lens ACS Survey (SLACS) and recent large-scale observations of galaxies, which is compiled and summarized in Cao et al. (2015) and Shu et al. (2017). The combined sample includes 91 lenses from SLACS (Bolton et al. 2008; Auger et al. 2009; Shu et al. 2017) and an extension of the SLACS survey known as 'SLACS for the Masses' (S4TM) (Shu et al. 2015, 2017), 35 lenses from the BOSS emission-line lens survey (BELLS) (Brownstein et al. 2012) and BELLS for GALaxy-Lyα EmitteR sYstemsGALLERY (BELLS GALLERY) (Shu et al. 2016a,b), 26 lenses from the Strong Lensing Legacy Survey (SL2S) (Sonnenfeld et al. 2013a,b), and five lenses from Lenses Structure and Dynamic (LSD) (Treu & Koopmans 2002; Koopmans & Treu 2003; Treu & Koopmans 2004). The advantage of this recently assembled lens sample, the detailed information of which is described and listed in Chen et al. (2019), lies in its well-defined observational selection criteria satisfying the assumption of spherical lens mass model. Fig. 1 shows the redshift distributions of the lensing systems used in our analysis. However, a statistical analysis requires a sample that is complete and has well-characterized, homogeneous selection criteria. Note that the lensing systems collected in this analysis are selected in very different manners. For instance, the SLACS, S4TM, and BELLS surveys, respectively, selected candidates from the spectroscopic observations of ETGs and look for the presence of higher redshift emission lines in Sloan Digital Sky Survey I (Eisenstein et al. 2001) and Sloan Digital Sky Survey-III (Eisenstein et al. 2011). These lens candidates were followed up with *HST* ACS snapshot imaging and after image processing. Therefore, in order to verify the completeness of the full early-type lens sample (hereafter Sample A), one additional subsample will also be applied to discuss its utility for the redshift test: 126 deflector-selected lenses from SLACS, S4TM, BELLS, and BELLS GALLERY (hereafter Sample B). Such choice is also motivated by the fact that the SLACS and BELLS lenses could be moderately suffered from the finite Sloan fibre size (Brownstein et al. 2012).

3 RESULTS

3.1 Constraints on the shape of VDF

We constrain the VDF of the form given by Equation (5) for the early-type VDF, which is well fitted by three effective parameters, i.e. the characteristic velocity dispersion (σ_*), the low-velocity power-law index (α), and the high-velocity cut-off index (β).[1] However, the strong lensing systems number statistics is not a strong enough test to enable the four-parameter function (Chae 2005). Hence, in order to break the parameter degeneracy without significantly altering the possible range of the VDF, we will focus on the constraints on shape of the VDF, with σ_* fixed at the best-fitting value by the SDSS DR5 local central stellar VDF (Choi et al. 2007)

$$(\sigma_*, \quad \alpha, \quad \beta)_{\rm DR5} = [161 \pm 5\,{\rm km\,s^{-1}}, \quad 2.32 \pm 0.10, \quad 2.67 \pm 0.07]. \tag{11}$$

The numerical results for the VDF shape parameters are summarized in Table 1, with the marginalized confidence limits (C.L.) on the parameter plane (α, β) presented in Fig. 1. Recent measurements of three stellar VDFs are also added for comparison: the VDF for local ETGs based on SDSS Data Release 5 (Choi et al. 2007), an inferred local stellar VDF obtained through Monte Carlo simulations, based on the galaxy luminosity functions from the SDSS and intrinsic correlations between luminosity and velocity dispersion (Chae 2010), and the VDF for quiescent galaxies in the local Universe, based on the Main Galaxy Sample from the SDSS Data Release 12 (Sohn, Zahid & Geller 2017).

In the first scenario, we assume that neither the characteristic velocity dispersion (σ_*) nor the number density (n_*) of galaxies evolves with redshifts ($\nu_n = \nu_v = 0$). Given the redshift coverage of the lensing galaxies in the lens sample ($0.06 < z_l < 1.0$), if we constrain a non-evolving VDF using the lens data, then, assuming the VDF evolution with redshift is smooth, the fits on the VDF parameters may represent the properties of ETGs at an effective epoch of $z \sim 0.5$. Such non-evolving VDF has been extensively applied in the previous studies on lensing statistics (Chae & Mao 2003; Ofek et al. 2003; Capelo & Natarajan 2007; Cao et al. 2012a). By applying the above-mentioned χ^2 – minimization procedure to Sample A – we obtain the best-fitting values and corresponding 1σ uncertainties (68.3 per cent confidence level): $\alpha = 0.66^{+2.13}_{-0.66}$, $\beta = 2.28^{+0.24}_{-0.18}$. It is obvious that the full sample analysis has yielded improved constraints on the high-velocity exponential cut-off index β, compared with the previous analysis of using the distribution of image separations observed in CLASS and PANELS to constrain a model VDF of ETGs (Chae 2005). Suffering from the limited size of lens sample, such analysis (Chae 2005) found that neither of the two VDF parameters (α, β) can be tightly constrained, due to the broad regions in the $\alpha - \beta$ plane. Consequently, the image separation distribution is consistent with the SDSS measured stellar VDF (Sheth et al. 2003) and the Second Southern Sky Redshift Survey (SSRS2) inferred stellar VDF (Chae & Mao 2003), although the two stellar VDFs are significantly different from each other concerning their corresponding parameter values. We also consider

[1]The characteristic number density (n_*) has no relation to the shape of lens redshift distribution, since a relative lensing probability as a function of z_l (see Equation 4) is used in this analysis, instead of the absolute lensing probability through Equation (1). This allows us to fix n_* by an arbitrary constant.

Table 1. Summary of the constraints on the shape of the model VDF of ETGs, based on the lens redshift distribution of the current strong lensing observations.

VDF Evolution	Data	σ_* (km s^{-1})	α	β
$\nu_n = \nu_v = 0$	Sample A	161	$0.66^{+2.13}_{-0.66}$	$2.28^{+0.24}_{-0.18}$
$\nu_n = \nu_v = 0$	Sample B	161	$1.00^{+2.38}_{-1.00}$	$2.34^{+0.26}_{-0.24}$
$\nu_n = -1.0$, $\nu_v = 0.25$	Sample A	161	$0.45^{+2.38}_{-0.45}$	$2.55^{+0.28}_{-0.20}$
$\nu_n = -1.0$, $\nu_v = 0.25$	Sample B	161	$0.70^{+2.63}_{-0.70}$	$2.55^{+0.30}_{-0.24}$
$\nu_n = \nu_v = 0$	Sample A	161 ± 5	$0.86^{+2.18}_{-0.86}$	$2.30^{+0.24}_{-0.20}$
$\nu_n = -1.0$, $\nu_v = 0.25$	Sample A	161 ± 5	$0.48^{+2.40}_{-0.48}$	$2.57^{+0.28}_{-0.21}$

constraints obtained for the Sample B (defined in previous section), with the likelihood is maximized at $\alpha = 1.00^{+2.38}_{-1.00}$ and $\beta = 2.34^{+0.26}_{-0.24}$, from which one could clearly see the marginal consistency between our fits and recent measurements of three stellar VDFs (especially the SDSS DR5 VDF of ETGs).

What would be an appropriate interpretation of this disagreement between the local stellar VDF and the lensing-based inferred VDF? In order to answer this question we must quantitatively examine the effects of the evolution in the VDF. Therefore, in the second model we adopt the number density and mass evolution in the ETG population from the recent studies of Faber et al. (2007) and Brown et al. (2007), which gave a decline in the abundance by roughly a factor of two ($\nu_n = -1$) and a 20 per cent increase in the velocity dispersion ($\nu_v = 0.25$) for ETGs from $z = 0$ to 1. Limits on the VDF shape parameters are also shown in Table 1 and Fig. 2. For Sample A, $\alpha = 0.45^{+2.38}_{-0.45}$ and $\beta = 2.55^{+0.28}_{-0.20}$ are obtained at 68.3 per cent confidence level, while the constraints on the individual VDF parameters are $\alpha = 0.70^{+2.63}_{-0.70}$ and $\beta = 2.55^{+0.30}_{-0.24}$ for Sample B. The main features of Fig. 2 may be summarized as follows. First, comparing constraints based on no-evolution and redshift-evolution models, one may clearly see that the VDF parameters obtained from the redshift-evolution model disagree with the respective value derived from no-evolution model at 1σ. More specifically, fits on the high-velocity cut-off index reveal the better consistency between the solely lensing-based VDF (assuming passive evolution) and the measured SDSS DR5 VDF of ETGs in the local Universe. Hence, the evolution of the VDF still significantly affects lensing statistics if the lensing galaxies are of early-type (Mitchell et al. 2005). Secondly, both of the SDSS DR5 and SDSS DR12 measured stellar VDFs agree very well with the lens redshift distribution, while the simulated local stellar VDF is disfavoured at high confidence levels ($>3\sigma$). Thirdly, it is of great importance to take into account the effects of sample incompleteness, given the lens redshift range of $0.234 < z_l < 1.00$ for Sample A (with the median value of $z_l = 0.268$) and $0.06 < z_l < 0.72$ for Sample B (with the median value of $z_l = 0.208$). Especially, for the Sample B we find that the lensing-based values of (α, β) are nearly equal to the corresponding stellar values for the adopted SDSS DR5 VDF in the redshift-evolution scenario. This is an argument in favour of the efficiency of lens redshift test as a probe of the VDF of ETGs. Therefore, our results indicate that sample selection plays an important role in determining the VDF shape of early-type population from the lens redshift test. Such findings, which highlight the importance of considering galaxy evolution and sample selection to better investigate the global properties of ETGs, have been extensively discussed in many previous works focusing on improved constraints on the cosmological parameters through strong lensing statistics (Cao et al. 2012a,b).

3.2 Constraints on the evolution of ETGs

Considering the redshift range of the lensing galaxies referring to the distant Universe (from $z = 0.06$ to $z = 1.0$), it is quite necessary to stress another question, that is: *Is it possible to achieve a stringent constraint on galaxy evolution by using gravitational lenses since redshift $z \sim 1.0$?* From this point of view, in the framework of the VDF for local ETGs based on SDSS Data Release 5 (Choi et al. 2007), we assume that the (characteristic) number density and velocity dispersion of lensing galaxies evolves as a function of redshift according to Equation (6).

Notice that the previous studies always considered only the evolution of the number density and the characteristic velocity dispersion, assuming a constant shape of the inferred VDF (Chae & Mao 2003; Ofek et al. 2003). In this analysis, the measured value of the two evolution parameters are $\nu_n = -1.18^{+3.04}_{-2.82}$ and $\nu_v = 0.18^{+0.21}_{-0.16}$ when the full lensing sample is taken into consideration. For Sample B, the best-fitting values and the 1σ limits change to $\nu_n = -1.56^{+4.01}_{-3.39}$, $\nu_v = 0.20^{+0.26}_{-0.22}$. Fig. 3 shows the constraints in the $\nu_n - \nu_v$ plane. On the one hand, our analysis reveals the strong degeneracy between the evolutions of the velocity dispersion and the number density, which is supported by the most degenerate direction in the evolution parameters (Oguri et al. 2012). On the other hand, the inferred evolutionary trends of the early-type VDFs are particularly interesting: lensing statistics demand that for early-type population at redshift $z = 1$, there should be a decline in the number density by a factor of two ($\nu_n \sim -1$) compared with the present-day value. This implies that dynamically, the population of lensing galaxies can be much different from the present-day population. Meanwhile, such change in number also requires a 20 per cent increase in the characteristic velocity dispersion ($\nu_v = 0.25$), following the general scenario of high-redshift formation and passive evolution of ETGs reported by the recent studies (Brown et al. 2007; Faber et al. 2007). We remark here that in the ΛCDM hierarchical structure formation picture, the dark halo mass function (DMF) and the VDF of galaxies evolve in cosmic time as a consequence of hierarchical merging (White & Rees 1978; Lacey & Cole 1993). In our analysis, the lensing-based VDF evolution is strikingly similar to the prediction of the CDM hierarchical structure formation paradigm, concerning the DMF from *N*-body simulations and the stellar mass function (SMF) predicted by recent semi-analytic models of galaxy formation. Interestingly, our results are particularly in conflict with the results of several galaxy surveys (Fontana et al. 2006; Pozzetti et al. 2007; Marchesini et al. 2009), which support the stellar mass-downsizing evolution of galaxies (apparently anti-hierarchical). The disagreement between the lensing constraints and galaxy survey results is more apparent when the large size difference between the samples is taken into consideration.

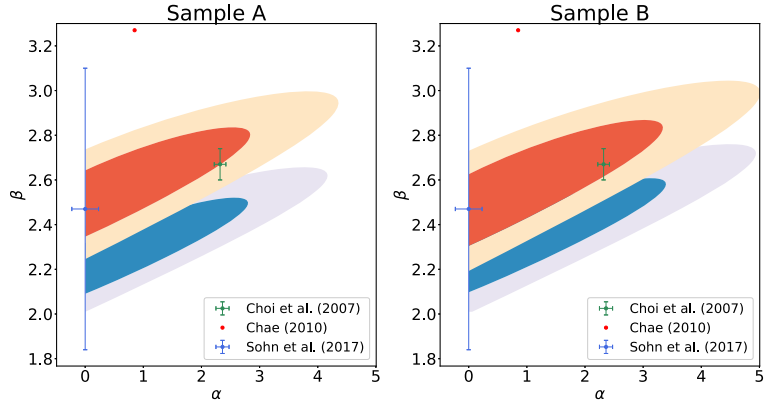

Figure 2. Constraints on the shape of the VDF, i.e. low-velocity power-law index α and high-velocity exponential cut-off index β with two lens samples (Sample A and Sample B), in the framework of no-evolution (blue contours) and redshift-evolution model (red contours).

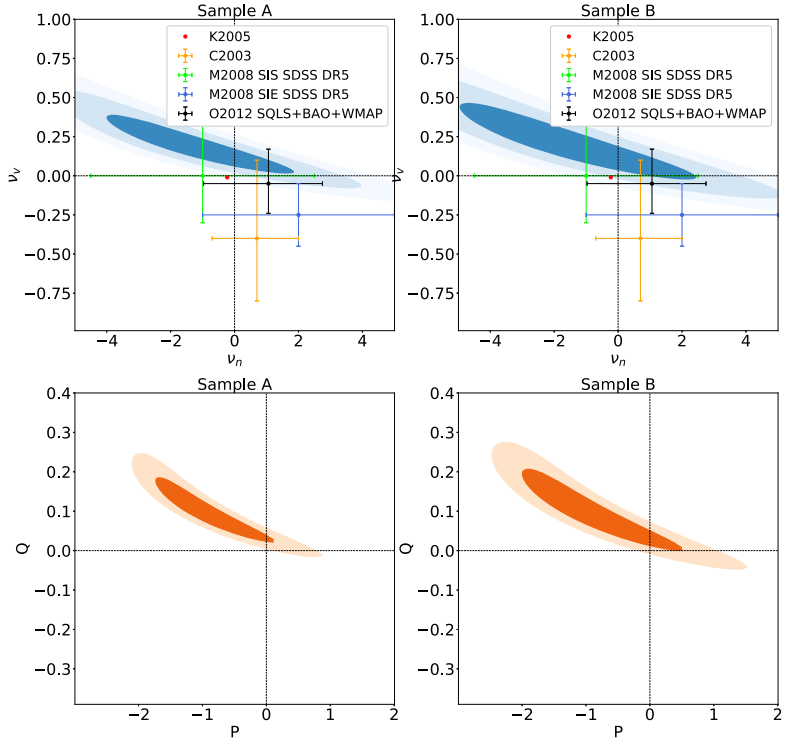

Figure 3. Constraints on the redshift evolution of the VDF, i.e. the number density evolution index ν_n (P) and the velocity dispersion evolution index ν_v (Q) with two different lens samples (Sample A and Sample B). The no-evolution model (black dashed lines) and the evolution parameters obtained in the literature are also added for comparison (see the text for more details).

One should bear in mind that the above results involve several uncertainties and assumptions that act as systematic errors in our analysis. Specifically, we consider the following sources of systematic errors in a similar way as done in Matsumoto & Furamase (2008) and Cao et al. (2012a). First, one possible source of uncertainties inherent to our analysis is the uncertainty of VDF parameters given by Equation (11). Therefore, based on the full lens sample, we vary the characteristic velocity dispersion by $\Delta\sigma_* = 5\,\mathrm{km\,s^{-1}}$ and obtain the constraints on the shape of early-type VDF in Table 1. Furthermore, while adopting the best-fitting VDF measurement in the SDSS DR5 as our fiducial model, we perform a sensitivity analysis and investigate how galaxy evolution is altered by introducing the uncertainties of α, β, and σ_*. The final results show that although the constraints become relatively weak due to the uncertain stellar VDF measurements in the local Universe, central fits are almost the same. Secondly, the parametrization of galaxy evolution is another important source of systematic error on the final results. Although this problem has been recognized long time ago, the most straightforward solution to this issue is focusing on other well-known evolution models, which have been widely used for analysis of statistical lensing in the previous works (Oguri et al. 2012). Consequently, in the following analysis we also perform fits on the second evolution model with a constant shape of the VDF. Specially, the velocity dispersion (as well as the number density) varies as a function of redshift (equation 7) (Ofek et al. 2003; Chae 2010). The simultaneous constraints on the redshift evolution of the VDF (P, Q) are shown in Table 2 and Fig. 3, with the best-fitting value of $P = -0.87^{+0.99}_{-0.86}$, $U = 0.09^{+0.09}_{-0.07}$ (Sample A) and $P = -0.88^{+1.39}_{-1.11}$,

Table 2. Summary of the constraints on the evolution parameters, based on the lens redshift distribution of the current strong lensing observations.

VDF parameters (σ_*, α, β)	Data	ν_n	ν_v
(161 km s^{-1}, 2.32, 2.67)	Sample A	$-1.18^{+3.04}_{-2.82}$	$0.18^{+0.21}_{-0.16}$
(161 $\pm$ 5 km s^{-1}, 2.32 $\pm$ 0.10, 2.67 $\pm$ 0.07)	Sample A	$-1.02^{+3.15}_{-2.74}$	$0.17^{+0.19}_{-0.16}$
(161 km s^{-1}, 2.32, 2.67)	Sample B	$-1.56^{+4.01}_{-3.39}$	$0.20^{+0.26}_{-0.22}$
VDF parameters (σ_*, α, β)	Data	P	Q
(161 km s^{-1}, 2.32, 2.67)	Sample A	$-0.87^{+0.99}_{-0.86}$	$0.09^{+0.09}_{-0.07}$
(161 km s^{-1}, 2.32, 2.67)	Sample B	$-0.88^{+1.39}_{-1.11}$	$0.09^{+0.11}_{-0.09}$

$Q = 0.09^{+0.11}_{-0.09}$ (Sample B). Again, our studies of galaxy evolution (based on the lens redshift distribution of Sample A and Sample B) still prefer a significant evolution in the number and mass of ETGs at $z \sim 1$.

4 DISCUSSIONS

In this paper, we have used the strong lensing statistics (i.e. the lens redshift distribution) of a well-defined sample of early-type gravitational lenses extracted from a large collection of 157 systems to constrain the VDF and the evolution of ETGs. By adopting a power-law model for galactic potentials and the cosmological parameters determined by the recent *Planck* observations, we employ the lens redshift test proposed in Kochanek (1992) and Ofek et al. (2003) to constrain the VDF of ETGs and its evolution in a more complicated model. Our results have shown that the population of ETGs can be much different from the present-day population (Section 3.1) and the lens redshift distribution is a sensitive probe of galaxy evolution (Section 3.2).

One important issue is the comparison of our results with the estimation of parameters in the power-law evolution model obtained in the previous studies (Chae & Mao 2003; Kang et al. 2005; Matsumoto & Furamase 2008; Oguri et al. 2012). This is illustrated in Fig. 3, which directly shows the evolution parameters obtained in this analysis and in the literature. The red dot circle denotes the best-fitting evolution parameters predicted by the semi-analytic model in Kang et al. (2005), while the orange cross represents the 1σ limits on the two evolutionary indices derived by the observed image separations of 13 lenses from CLASS (Chae & Mao 2003). The green and blue crosses show the results (1σ uncertainties) with the WMAP's best-fitting ΛCDM cosmology (Matsumoto & Furamase 2008), concerning the lens-redshift test of the well-defined SDSS lens sample characterized by different galaxy mass profiles (SIS and SIE lens for SDSS DR5). The black cross denotes the recent measurements of the redshift evolution of VDF based on the statistical analysis of the final sample from SQLS, combined with external cosmological probes such as BAO and WMAP (Oguri et al. 2012). We obtain the constraints on the evolution of the characteristic number density and velocity dispersion which are in broad agreement with these previous studies (especially the SIS lenses for SDSS DR5) (Matsumoto & Furamase 2008). We also compare our results with recent fits obtained in recent measurements of the SMF, based on the examination of galaxy populations at $z \sim 1$. More specifically, although the effects of the redshift evolution form has yet to be fully clarified, it was found in Ilbert et al. (2010), Matsuoka & Kawara (2010), and Brammer et al. (2011) that the number density of galaxies for a given stellar mass range can evolve by a factor of two from $z = 0$ to 1. Further papers have also noticed such redshift evolution in the direct evolution measurement of the velocity function (up to $z \sim 1$), focusing on a scaling relation between velocity dispersion, stellar mass, and galaxy structural properties (Bezanson et al. 2011). The above findings are in fact compatible with our results based on the strong lensing statistics (i.e. the redshift distribution of galactic-scale lenses).

The importance of galaxy evolution in strong lensing statistics was also widely recognized (Chae & Mao 2003; Chae 2010; Oguri et al. 2012). Such evolution scenario of ETGs, which coincides with the recent studies of the Fundamental Plane of lensing galaxies (Kochanek et al. 2000; Rusin et al. 2003), is different from that obtained in Chae & Mao (2003), with the best-fitting value of ν_n being positive and ν_v being negative in the hierarchical structure formation theory. Our different conclusion might be due to the fact that our lens sample is extended to a wide coverage of velocity dispersions (98 km s^{-1} $\leq \sigma \leq$ 396 km s^{-1}). As was found in the recent analysis of the early-type VDFs from $z = 1$ to $z = 0$ (Matsumoto & Furamase 2008; Chae 2010), the differential number density of ETGs would experience greater evolution at a higher velocity dispersion. Specially, an increasingly large factor ($\geq$3) was reported for the galaxies at the largest velocity dispersion end ($\sigma \geq 300$ km s^{-1}) since $z = 1$ (Chae 2010). However, the lens sample used by the previous lensing statistics is restricted to ETGs with typical velocity dispersions and lower ($\sigma \leq 230-250$ km s^{-1}), for which there is no statistically significant change in number density from $z = 0$ to $z = 1$ (Oguri et al. 2012). This explains why the no-evolution of the early-type population, which has usually been used to constrain cosmological parameters and test the properties of dark energy, appears to be supported by different strong lensing statistics (Chae 2005; Mitchell et al. 2005). On the other hand, the lens sample used in this analysis is more complete in the source and lens redshifts, with a better understanding of the selection function than that adopted in Chae & Mao (2003) and Chae (2005).

Most studies of strong lensing statistics have used the galaxy population with constant VDF shape for the number density of lenses (Chae & Mao 2003; Ofek et al. 2003; Chae 2005; Matsumoto & Furamase 2008; Cao et al. 2012a). Following the recent results indicating the differential redshift evolution in the number density of galaxies with different velocity dispersions (Bezanson et al. 2012; Montero-Dorta et al. 2017), we also include an additional parameter k_β to describe the redshift evolution of the shape of the velocity function (Chae 2010)

$$\alpha \rightarrow \alpha \left(1 + k_\beta \frac{z_l}{1+z_l}\right), \ \beta \rightarrow \beta \left(1 + k_\beta \frac{z_l}{1+z_l}\right). \quad (12)$$

$k_\beta > -1$ is required to guarantee the positivity of the VDF shape parameters (α, β). Note that such additional parametrization, which is well consistent with the intermediate-redshift VDFs steeper both at the low-velocity and high-velocity ends (Oguri et al. 2012), could also effectively describe the redshift dependence of the halo-mass function suggesting stronger redshift evolution for larger velocity dispersions (Mitchell et al. 2005; Matsumoto & Furamase 2008). The constrains on individual evolution parameters are presented in Fig. 4. It should be stressed that in the framework of a more complicated model, the evolution of the VDF shape and the 1σ limits is $k_\beta = -0.25^{+0.17}_{-0.29}$ for the full lensing sample, which is marginally consistent with the fiducial no-redshift-evolution case ($k_\beta = 0$). However, the correlation between k_β and (ν_n, ν_v) is apparently indicated in our analysis, i.e. a significant evolution of the VDF shape will lead to a smaller value for the (characteristic) number density evolution and a larger value for the velocity dispersion evolution of lensing galaxies.

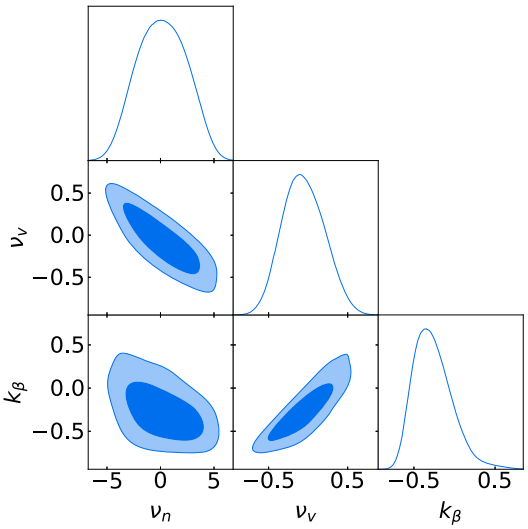

Figure 4. Constraints on the redshift evolution of the VDF in a more complicated evolution model with the full lens sample (Sample A). The additional parameter k_β is included to quantify the evolution of the VDF shape.

As a final remark, we point out that the lensing constraints on the VDF and the evolution of ETGs are quite competitive, compared with those from other methods such as redshift survey of galaxies. However, our analysis still potentially suffers from the limited size of the lens sample. Meanwhile, strong lensing systems with high-redshift quasars ($z \sim 5$) acting as the background source will dramatically contribute to investigating the effects of galaxy evolution on the lens statistics, as was found in the recent works of Chae & Mao (2003). With planned upgrades in next generation of wide and deep sky surveys (such as the Large Synoptic Survey Telescope, LSST), it is possible to discover 10^5 galactic-scale lenses in the near future, with the corresponding source redshift reaching to $z \sim 6$ (Collett 2015).

For this purpose we create mock data including 10^4 strong lensing systems on the base of realistic population models of elliptical galaxies acting as lenses. Construction of the mock catalogue proceeded along the following steps (Cao et al. 2019, 2020): (i) For the purpose of calculating the sampling distribution (number density) of lenses, we use the VDF of elliptical galaxies in the local Universe derived from SDSS Data Release 5 (Choi et al. 2007). Meanwhile, in our simulation we assume that neither the shape nor the normalization of this function vary with redshift. The lens redshift of our simulated sample, whose distribution is well approximated by a Gaussian with mean $z_l = 0.45$ and well consistent with the properties of the SL2S sample, could reach to $z_l \sim 2$ (Liu et al. 2020a,b). (ii) The lens mass distribution is approximated by the singular isothermal ellipsoids, while the simulated population of lenses is dominated by galaxies with velocity dispersion of $\sigma_0 = 210 \pm 50$ km s^{-1}. (iii) The three angular diameter distances of the lensing systems (from observer to lens, from observer to source, and from lens to source) are calculated in the framework of a fiducial cosmological model (ΛCDM) from recent *Planck* observations (Ade et al. 2016). The effectiveness of our method could be seen from the discussion of this question: *Is it possible to achieve a stringent measurement of the evolution of early-type galaxies?* In the framework of a generalized evolution model given the evolution of VDF shape, one can expect the evolutions of the number density and the characteristic velocity dispersion to be estimated with the precision of $\Delta\nu_n = 0.085$ and $\Delta\nu_v = 0.006$. The resulting constraint on the redshift evolution of the VDF shape becomes $\Delta k_\beta = 0.012$, when the differential redshift evolution in the number density of galaxies with different velocity dispersions is taken into consideration. Now the final question is *Is it possible to confirm or falsify alternative semi-analytic models of galaxy formation?* In particular, many galaxy surveys suggest stellar mass-downsizing (apparently anti-hierarchical) evolution of galaxies (Fontana et al. 2006; Pozzetti et al. 2007; Marchesini et al. 2009), although there are results that do not particularly support such evolution scenario (Brown et al. 2007; Faber et al. 2007). The most striking conclusion of these works is the emergence of the considerable evolutions of the number density and the characteristic velocity dispersion, i.e. $(\nu_n, \nu_v) = (-1, 0.25)$ for hierarchical model. Given the fact that the precision is inversely proportional to the $\sqrt{N}$ (where N is the number of systems), with 10^4 strong lensing systems one can effectively differentiate between the hierarchical and anti-hierarchical models at very high confidence $>5\sigma$. Summarizing, when such a lens sample – which increases the current lens size by orders of magnitude – is available, one could expect the most stringent lensing constraints on the formation and evolution of ETGs, from the redshift distribution of gravitational lenses.

ACKNOWLEDGEMENTS

This work was supported by National Key R&D Program of China No. 2017YFA0402600; the National Natural Science Foundation of China under Grants Nos. 12021003, 11690023, 11633001, and 11920101003; Beijing Talents Fund of Organization Department of Beijing Municipal Committee of the CPC; the Strategic Priority Research Program of the Chinese Academy of Sciences, Grant No. XDB23000000; the Interdiscipline Research Funds of Beijing Normal University; and the Opening Project of Key Laboratory of Computational Astrophysics, National Astronomical Observatories, Chinese Academy of Sciences. This work was initiated at Aspen Center for Physics, which is supported by National Science Foundation grant PHY-1607611. This work was partially supported by a grant from the Simons Foundation. M. Biesiada is grateful for this support.

DATA AVAILABILITY STATEMENTS

The data underlying this article will be shared on reasonable request to the corresponding author.

REFERENCES

Abazajian K. N. et al., 2009, ApJS, 182, 543
Ade P. A. R. et al., 2016, A&A, 594, A13
Auger M. W. et al., 2009, ApJ, 705, 1099
Bernardi M. et al., 2010, MNRAS, 404, 2087
Bezanson R. et al., 2012, ApJ, 760, 62
Bezanson R. et al., 2011, ApJ, 737, L31
Biesiada M., 2006, Phys. Rev. D, 73, 023006
Bolton A. S. et al., 2008, ApJ, 682, 964
Brammer G. B. et al., 2011, ApJ, 739, 24
Brown M. J. I., Dey A., Jannuzi B. T., Brand K., Benson A. J., Brodwin M., Croton D. J., Eisenhardt P. R., 2007, ApJ, 654, 858
Brownstein et al., 2012, ApJ, 744, 41
Cao S. et al., 2012a, ApJ, 755, 31
Cao S. et al., 2012b, J. Cosmol. Astropart. Phys., 03, 016
Cao S. et al., 2012c, A&A, 538, A43
Cao S. et al., 2015, ApJ, 806, 185
Cao S. et al., 2016, MNRAS, 461, 2192

Cao S., Qi J., Cao Z., Biesiada M., Li J., Pan Y., Zhu Z.-H., 2019, Sci. Rep., 9, 11608
Cao S. et al., 2020, ApJ, 888, L25
Cao S. et al., 2021, MNRAS, 502, L16
Capelo P. R., Natarajan P., 2007, New J. Phys., 9, 445
Chae K.-H., 2005, ApJ, 630, 764
Chae K.-H., 2007, ApJ, 658, L71
Chae K.-H., 2010, MNRAS, 402, 2031
Chae K.-H., Mao S., 2003, ApJ, 599, L61
Chen Y., Li R., Shu Y., 2019, MNRAS, 488, 3745
Choi Y.-Y. et al., 2007, ApJ, 658, 884
Cole S. et al., 1994, MNRAS, 271, 781
Collett T. E., 2015, ApJ, 811, 20
Eisenstein D. J. et al., 2001, AJ, 122, 2267
Eisenstein D. J. et al., 2011, AJ, 142, 72
Faber S. M. et al., 2007, ApJ, 665, 265
Fontana A. et al., 2006, A&A, 459, 745
Ilbert O. et al., 2010, ApJ, 709, 644
Jing Y. P., Suto Y., 2002, ApJ, 574, 538
Kang X. et al., 2005, ApJ, 631, 21
Kauffmann G., 1996, MNRAS, 281, 487
Kauffmann G., White S. D. M., Guiderdoni B., 1993, MNRAS, 264, 201
Keeton C. R., Kochanek C. S., 1997, ApJ, 487, 42
Keeton C. R., Kochanek C. S., Falco E. E., 1998, ApJ, 509, 561
Kochanek C. S. et al., 2000, ApJ, 543, 131
Kochanek C. S., 1992, ApJ, 384, 1
Koopmans L. V. E., Treu T., 2003, ApJ, 583, 606
Koopmans L. V. E. et al., 2009, ApJ, 703, L51
Koopmans L. V. E., 2005, in Mamon G. A., Combes F., Deffayet C., Fort B., eds, Proceedings of XXIst IAP Colloquium, 'Mass Profiles & Shapes of Cosmological Structures', EDP Sciences, France
Lacey C, Cole S., 1993, MNRAS, 262, 627
Liu T. H. et al., 2020a, ApJ, 899, 71
Liu T. H. et al., 2020b, MNRAS, 496, 708
Marchesini D. et al., 2009, ApJ, 701, 1765
Matsumoto A., Futamase T., 2008, MNRAS, 384, 843
Matsuoka Y., Kawara K., 2010, MNRAS, 405, 100
Mitchell J. L. et al., 2005, ApJ, 622, 81
Montero-Dorta A. D., Bolton A. S., Shu Y., 2017, MNRAS, 468, 47
Ofek E. O., Rix H.-W., Maoz D., 2003, MNRAS, 343, 639
Oguri M. et al., 2012, ApJ, 143, 120
Pan Y. et al., 2016, Int. J. Mod. Phys., 25, 1650003
Pozzetti L. et al., 2007, A&A, 474, 443
Qi J.-Z. et al., 2019, Phys. Rev. D, 100, 023530
Renzini A., 2006, ARA&A, 44, 141
Rusin D. et al., 2003, ApJ, 587, 143
Sheth R. K. et al., 2003, ApJ, 594, 225
Shu Y. et al., 2015, ApJ, 803, 71
Shu Y. et al., 2016a, ApJ, 824, 86
Shu Y. et al., 2016b, ApJ, 833, 264
Shu Y. et al., 2017, ApJ, 851, 48
Sohn J., Zahid H. J., Geller M. J., 2017, ApJ, 845, 73
Sonnenfeld A. et al., 2013a, ApJ, 777, 97
Sonnenfeld A. et al., 2013b, ApJ, 777, 98
Treu T. et al., 2006, ApJ, 640, 662
Treu T., Koopmans L. V. E., 2002, ApJ, 575, 87
Treu T., Koopmans L. V. E., 2004, ApJ, 611, 739
Turner E. L. et al., 1984, ApJ, 284, 1
White S. D. M., Rees M. J., 1978, MNRAS, 183, 341

This paper has been typeset from a TEX/LATEX file prepared by the author.